

Cyclic caldera collapse: Piston or piecemeal subsidence? Field and experimental evidence

V.R. Troll*

T.R. Walter

H.-U. Schmincke

Abteilung für Vulkanologie und Petrologie, GEOMAR Forschungszentrum,
Wischhofstrasse 1-3, 24148 Kiel, Germany

ABSTRACT

Many multicycle caldera volcanoes display a complex extracaldera fault system genetically linked to caldera evolution. On Gran Canaria (Canary Islands), the Miocene Tejeda caldera was filled by ignimbrites and epiclastic sediments and intruded by syenites and a major cone-sheet swarm, obscuring intracaldera structural relations. Extracaldera radial and circumferential faults and dikes are well exposed. We used field data and experiments scaled to the island of Gran Canaria to clarify the poorly understood structural, temporal, and genetic relationship of peripheral faults to the central caldera. The experimental setup comprises a cone of medium-grained sand in which a rubber balloon was repeatedly inflated and deflated. Balloon inflation resulted in updoming and a dominantly radial fault pattern, whereas balloon deflation caused piecemeal caldera collapse and a concentric peripheral fault arrangement on the edifice flanks. A complex interplay of repeated inflation and deflation cycles of the experimental magma chamber is found to explain the peripheral fault system of the Tejeda caldera on Gran Canaria and offers insight into the structure of the caldera floor and the mechanisms acting in multicycle caldera volcanoes.

Keywords: multicycle caldera volcanoes, analogue experiments, Tejeda caldera, Gran Canaria.

INTRODUCTION

Calderas probably form by decompression of a shallow-level magma chamber, followed by roof collapse into the evacuating reservoir (Smith and Bailey, 1968; Druitt and Sparks, 1984; Lipman, 1997). Different styles of gravitational subsidence suggested include piston collapse, noncoherent (piecemeal) collapse, down-sag, and funnel collapse (Lipman, 1997). Experimental and theoretical studies show that the structural evolution and the subsidence mechanisms of an individual caldera depend on the initial structure of the volcano, the presence and/or absence of regional tectonic influence, the size, depth, and shape of the underlying magma chamber, and the eruptive magnitude and intensity of the pressure variation within the magma chamber (Komuro, 1987; Gudmundsson, 1988; Marti et al., 1994, 2000; Roche et al., 2000; Acocella et al., 2000; Walter and Troll, 2001). Two main collapse mechanisms have been proposed; piecemeal collapse and piston cylinder subsidence (Lipman, 1997), the former being thought to be much less important than the latter. Here we demonstrate that extracaldera structural relationships on Gran Canaria and analogue modeling argue for piecemeal evolution of multicyclic calderas to be more common than previously thought. The type of evidence as-

sembled overcomes the common difficulty in distinguishing between different structural processes because many young calderas are filled by thick ignimbrite sequences and/or are obscured by postcaldera intrusions.

On Gran Canaria (Canary Islands), a major Miocene multicycle caldera is filled with ignimbrites and sediments, but displays a complex extracaldera (peripheral) structural system of radial and concentric dikes and faults (Schmincke, 1976). This type of peripheral structure is a common phenomenon in multicycle caldera systems (e.g., Varnes, 1963; Smith and Bailey, 1968; Gardeweg and Ramirez, 1987; Newhall and Dzurisin, 1988; Henry and Price, 1989; Nappi et al., 1991), but its origin and relationship to the ring fault and intracaldera structure remain poorly understood. In order to evaluate the structural implications of fault systems peripheral to calderas, we combine field evidence on Gran Canaria with scaled analogue experiments simulating a multicycle caldera volcano. A comparison of the fault and dike distribution of the Tejeda caldera with the experimental results helps us to understand the origin of the Tejeda caldera and its peripheral fault structure. The results are applicable to caldera periphery fault systems of multicycle calderas elsewhere.

FIELD OBSERVATIONS

A well-exposed outer caldera margin on Gran Canaria (Fig. 1) separates the Miocene

basaltic shield lavas overlain by felsic extracaldera ignimbrites from intracaldera ignimbrites, sediments, and intrusives (Schmincke and Swanson, 1966; Schmincke, 1967). The caldera formed as a result of more than 20 trachytic to rhyolitic ignimbrites between 14 and 13.2 Ma (Mogan Group) and many trachyphonolitic ignimbrites and lava flows between 13.2 and 8.5 Ma (Fataga Group) (Schmincke, 1976; Bogaard and Schmincke, 1998). Correlation of intracaldera ignimbrites with the extracaldera ignimbrite succession suggests at least 1 km subsidence of the caldera basin (Schmincke, 1967). The caldera fill was intruded by syenites and a cone-sheet swarm of more than 500 trachytic to phonolitic sheets, emplaced between 12.3 and 7.3 Ma, representing late resurgence of the Tejeda caldera (Schmincke et al., 1999). Due to lack of exposed caldera basement and the obscured nature of the intracaldera structural relations, information on the caldera-forming mechanism(s) is best preserved at the caldera margin and the extracaldera periphery fault system.

The topographic caldera margin dips 50°–80° inward, whereas shield basalts and the ignimbrite succession dip gently toward the sea. Tuffs and sediments that fill the caldera pinch out against the steep caldera margin. An up-section decrease in the dip of depositional bedding indicates progressive filling of the caldera. At deeper levels the caldera margin

*E-mail: trollv@tcd.ie.

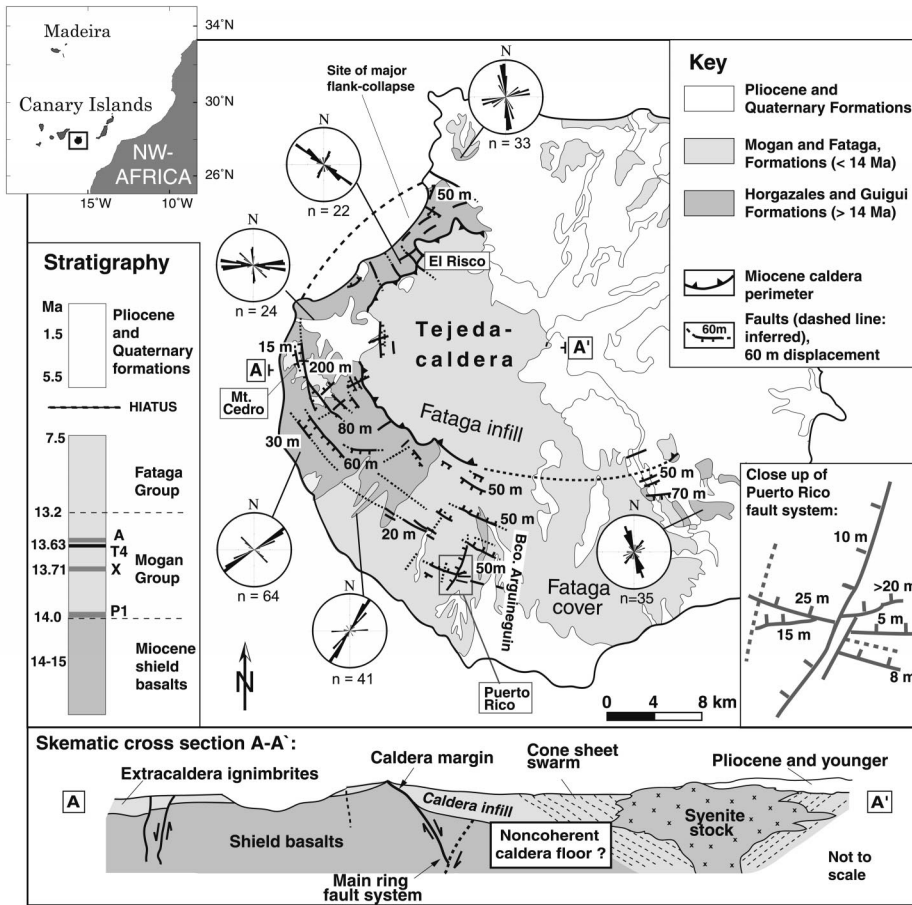


Figure 1. Map of Gran Canaria showing caldera and peripheral fault distribution. Equal-area pole plots (axial with class interval of 5°, n = number of data) represent dike orientations at given locality with radial and concentric trends throughout caldera periphery. Inset lower left shows major stratigraphic units of Gran Canaria. Lower right inset is closeup of Puerto Rico fault system showing intersecting radial and concentric faults of several generations. Bottom inset is schematic cross section through Gran Canaria as indicated (A-A').

increasingly steepens, reaching vertical orientation in the deeply dissected erosional valley of El Risco in the northwest of the island. Here, but at a higher stratigraphic level, the caldera margin shallows to an inward dip of only 40°–50°, suggesting a curved caldera margin, progressively shallowing toward the former land surface. Whether the observed caldera margin represents only the outer erosional limit of the caldera basin or is actually a fault remains speculative. However, the curvature of the contact may suggest a gradation from an erosional margin higher up the contact to a fault origin at depth.

Several generations of radial and concentric faults outside the caldera margin can be correlated to several episodes of volcanic activity. Radial dikes comprise pre-ignimbrite Miocene shield basalts, early Mogan rhyolites, and Fataga alkalic basalts and phonolites. Radial dikes and faults occur from the caldera margin to the island coast and crosscut, and are crosscut by concentric caldera rim-parallel faults. The concentric faults form a complex system

of local horst and graben structures to 10 km outside the caldera margin (Fig. 1).

For example, the concentric Montaña Cedro fault zone in the southwest of the island, ~5 km from the caldera margin, shows a relative downthrow of the outer flank of the island, defining a large horst between the fault zone and the caldera rim. Particular marker ignimbrites, such as ignimbrite A, show substantial thickening to the west of the fault ($A > 25$ m), compared to the eastern, more proximal side to the caldera, where A is ≤ 10 m thick but vertically displaced by ~200 m. Stratigraphic units below ignimbrite A, however, show a reverse thickness relationship on either side of the fault; e.g., ignimbrite X is ~60 m thick on the eastern side, but ~20 m thick on the western side of the fault and displaced by only ~90 m. The fault zone is strongly brecciated and filled by Mogan-type basalt, rhyolite, and trachyte, plus Fataga phonolite fragments dragged into the fault. The fault was thus active during several eruptive episodes. This repeated fault activity differs from that of a sim-

ple growth fault, and is realistically only accomplished by multiple reactivation of the fault with opposing senses of displacement.

Many additional examples of complex, caldera margin-parallel faults displace the post-shield ignimbrite succession in the south of the island. In Arguineguin valley, ~3–6 km from the caldera margin, subparallel concentric faults define horst and graben structures of several hundred meters to 2 km in width. These uplifted and subsided blocks displace the lower units of the ignimbrite succession but leave upper units increasingly undisturbed, thus representing a system of repeatedly reactivated syncaldera faults.

The interplay of radial and concentric faults is well preserved, e.g., in Puerto Rico erosional valley, where a local concentric graben is intersected by a radial fault zone, producing a mosaic of smaller blocks. Within the graben, ignimbrite A is >30 m thick and shows its full sequence of 7 flow units. Beyond the graben, A is ≤ 10 m thick and the lower flow units are missing. There, along the radial fault, displacement of ignimbrite X shows a downthrow of ~15 m to the west. The overlying basalt flow T4 (that underlies A) is ~5 m thick on the downthrown side, but reaches ~15 m thickness on the uplifted eastern side of the radial fault. This implies several reactivations of radial and concentric faults to accumulate lava and ignimbrite within local grabens, some of which became uplifted blocks with extreme thicknesses of individual units. Evidence for multiple reactivation of once-formed syncaldera radial and concentric fault zones is therefore overwhelming in the periphery of the Gran Canaria caldera.

EXPERIMENTS

The experimental setup consists of a basement and cone of medium-grained sand, between which a latex balloon was placed. The balloon was connected with a pipe system to an external water reservoir; water input simulated magma chamber inflation and caused tumescence, while water withdrawal, and simulated chamber evacuation, led to subsidence of the chamber roof. Experiments obey the principle of similarity (see Komuro, 1987; Roche et al., 2000). The ratios of physical parameters (X) are determined by $X^* = X_{\text{Model}}/X_{\text{Nature}}$. The geometric proportions of the model were scaled to Gran Canaria Island, where a shallow ellipsoidal magma reservoir is postulated at 6–7 km depth with a diameter of ~17 km (Freundt and Schmincke, 1995; Ye et al., 1999; Krastel and Schmincke, 2001). Our scaling factor was $X^* = 10^{-5}$, so that 1 cm in the model corresponds to ~1 km in nature (Table 1). The slope of the cone was initially 10° with a flattened apex and a total height of the setup of 14–16 cm.

TABLE 1. GEOMETRIC RELATIONS OF EXPERIMENTS VERSUS GRAN CANARIA

Scaled Parameters (1:100 000)	Experiment (after cycle 1)	Experiment (after cycle 2)	Gran Canaria (multicyclic)
Magma chamber diameter	17 cm	17 cm	~17 km
Magma chamber depth	6 cm	6 cm	~6 km
Angle of internal friction	40°	40°	35°–45°
Radial crack or dike diameter	24 cm	28 cm	~32 km
Ring fault diameter	16 cm	20 cm	18–20 km
Ring fault subsidence	0.6 cm	1 cm	>1 km
Concentric periphery faults (maximum diameter)	25 cm	29 cm	~30 km
Periphery horst/graben blocks	2–4 cm	2–4 cm	1–4 km
Apical graben blocks	1–3 cm	2 cm	?
Apical graben subsidence	0.7 cm	0.8 cm	?

Crustal rocks and sand are Coulomb materials with a shear stress (τ) that depends on the material's cohesion (c), the normal stress (σ_n), and the angle of internal friction (ϕ), with $\tau = c + \sigma_n \tan \phi$. The granular sand used had a mean grain diameter of 300 μm , a density of $\rho_{\text{Model}} = 1300 \text{ kg m}^{-3}$, and an angle of internal friction of $\phi_{\text{Model}} = 33^\circ$, permitting simulation of brittle behavior of natural rocks (Hubbert, 1951), with $\rho_{\text{Nature}} = 2700 \text{ kg m}^{-3}$, $\phi_{\text{Nature}} = 25^\circ\text{--}40^\circ$ and $g_{\text{Nature, Model}} = 10$

ms^{-2} . The stress ratio (σ^*) is defined by the ratios of the length (L^*), the gravity acceleration (g^*), and the density (ρ^*), with $\sigma^* = \rho^* g^* L^* = 5 \times 10^{-6} \text{ Pa}$. Natural rocks cover a range of cohesive strength from $5 \times 10^7 \text{ Pa}$ to 10^6 Pa . The lower cohesion resembles strength values on larger scales and/or in fractured materials that contain cohesion-reducing discontinuities (see Roche et al., 2000). From the stress ratio σ^* that equals c^* follows a required cohesion for the analogue material of

$C_{\text{Model}} = C^* \times C_{\text{Nature}} = 5 \text{ Pa}$; a stress approximation using low cohesive sand was, therefore, suitable.

Cohesion in sand depends on its compaction, so that stressed and faulted sand has a lowered cohesion, allowing faults to become reactivated (Krantz, 1991). Limitations of the setup, however, include the tensile strength of the granular material, timing, gravity acceleration, and the size and shape of the chosen latex balloon. The latter is considered merely as an approximation, because the dimensions of natural reservoirs commonly remain speculative. Moreover, an inflated latex balloon with known shape produces on evacuation artificially reduced fault displacement near the balloon membrane. This is because fault propagation and sinking of roof blocks into the reservoir is hindered by the balloon membrane. In our experiments, balloon inflation raised the summit by 1–2 cm and steepened the flank by $\sim 10^\circ$. This inflation rate may somewhat overestimate the effects of a single natural inflation event. However, natural caldera volcanoes with domal uplift of 1000 m and more are known (Komuro, 1987; Troll et al., 2000). The fault pattern produced did not depend on the rate of doming, only the displacement and length of the faults diverged.

Experimental Results

During balloon inflation, open radial cracks formed and propagated divergently from the center outward, reaching a length of $\sim 12 \text{ cm}$ (Fig. 2; Table 1). Fracturing decreased from the free surface downward, as seen in experiments next to a glass pane. Simultaneously, the summit region extended laterally, producing polygonal concentric cracks that limited an apical graben. The formation of the apical graben included inward tilting and sagging of 1–3 cm blocks with normal fault subsidence of as much as 1 cm. The graben interior was strongly dissected by radial faults (Komuro, 1987). A small set of reverse concentric (inward dipping) faults formed on the flanks of the dome, with a relative uplift of the material closer to the center.

Subsequently, we deflated the balloon, causing synchronous surface sagging of the central region of the dome, followed by a slightly delayed caldera collapse. Within a radius of 8 cm, a set of vertical to steeply outward dipping ring faults formed, with as much as 0.6 cm fault displacement, resulting in non-coherent caldera-floor subsidence that was controlled by intersecting preexisting radial faults and newly formed concentric faults. The most significant vertical displacement was at the ring faults. At depth, coherence of the subsided roof increased due to reduced fault displacement closer to the balloon membrane, preventing fault propagation into the reservoir.

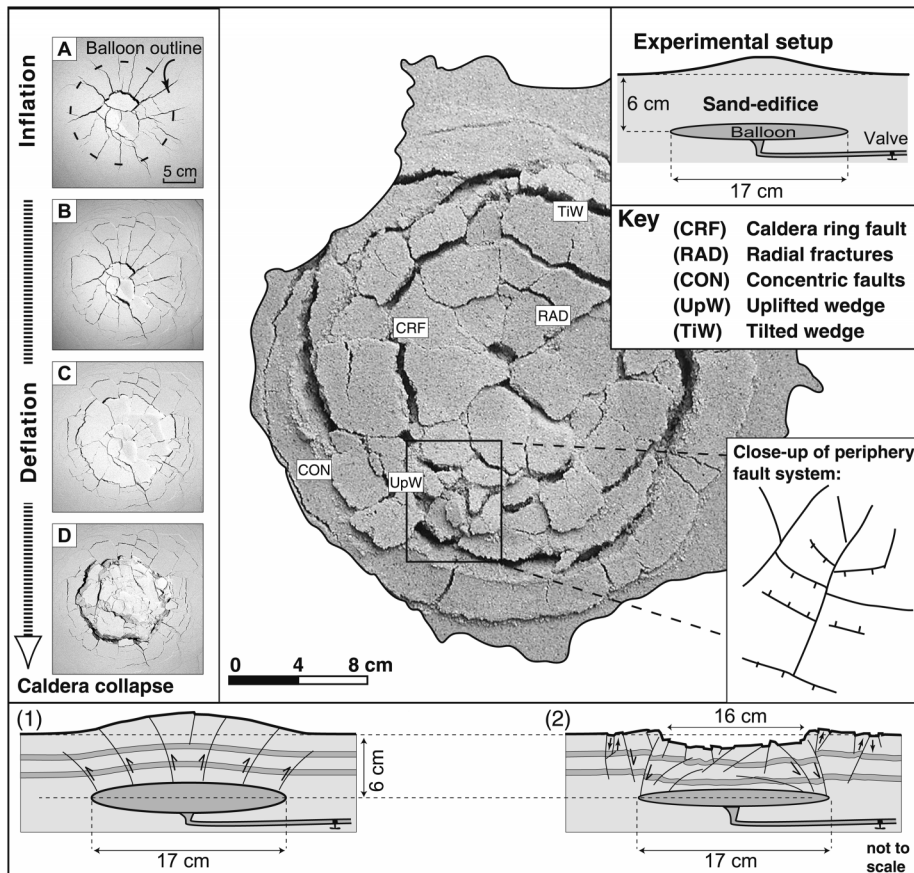


Figure 2. Experimental setup and results. Inset top right shows initial experimental construction prior to chamber inflation. Inset left shows photographs taken from above experimental setup after (A) inflation, (B, C) subsequent moderate deflation, and (D) evacuation of $\sim 75\%$ of balloon volume. Center: Photograph of surface deformation after cyclic inflation and deflation, projected onto outlines of Gran Canaria. Inset lower right: Close-up of complex fault interplay in periphery of produced caldera structure. Bottom inset: Cross sections of characteristic structures that form during balloon inflation (1) and subsequent balloon evacuation (2).

Outside the caldera, the flanks tilted inward followed by formation of a concentric fault pattern spanning the entire central caldera basin in an echelon fashion with a radius of 12.5–13 cm (Fig. 2). These faults were vertical to outward dipping and intersected the pre-existing radial doming structures on the flanks. Local horst and graben structures with blocks of 2–4 cm formed between concentric en echelon faults in the periphery and at the intersection of crosscutting radial and concentric faults in both the periphery and in the caldera.

Further cycles of inflation and deflation produced only subordinate new fractures but dominantly reused the preexisting faults in normal and reverse sense. These multicyclic experiments caused a widening of the central caldera basin by inward slumps from the steep ring fault and increased the radius of radial cracks on repeated doming. Horst and graben structures in the periphery also became reactivated and individual blocks were frequently uplifted during one stage of a cycle to become subsided grabens in another stage of the same cycle.

A circular collapse basin with only circular ring faults, lacking radial faults (piston cylinder), was only observed in some pure chamber evacuation experiments, i.e., without any precollapse or postcollapse tumescence (Marti et al., 1994; Roche et al., 2000). Peripheral horst and graben structures, in turn, were not produced during pure chamber evacuation runs.

DISCUSSION

On Gran Canaria, radial and concentric caldera periphery faults were active during multicycle ignimbrite eruptions and corresponding caldera evolution. The concentric periphery fault zone is not a single sharply defined circular fault; rather, it forms a set of steeply dipping fault segments including horst and graben structures and large concentric horst structures between the concentric periphery zone and the caldera margin (Fig. 1). Reactivation of radial faults, episodic radial dike emplacement, and reactivation of concentric horst and graben structures was common and produced repeated differential uplift or subsidence of individual blocks according to the local stress pattern. Field observations on Gran Canaria are consistent with our experimental results, and the comparison of nature and experiment strongly resembles a series of structural features and proportions (Table 1).

The similarities between Gran Canaria and the scaled experiments suggest that the floor of the Tejeda caldera and the lower caldera infill are controlled by radial faults that crosscut, and are crosscut by, concentric faults. However, they are now largely covered by

younger deposits and obscured by intrusives. The inference of intracaldera crosscutting radial and concentric fractures on Gran Canaria is consistent with observations by Schirnick (1996), who found crosscutting radial and concentric dikes of Mogan age in a deeply eroded valley that cuts into the intracaldera succession. The existence of crosscutting radial and concentric faults and dikes in the caldera periphery, in the intracaldera succession, and in the experiments, strongly implies that multicycle calderas, such as Tejeda caldera on Gran Canaria, are unlikely to have undergone simple piston-type collapse. We suggest discrete block subsidence (i.e., piecemeal) to be the major subsidence mechanism in such long-lived caldera systems. Combining experimental and field observations, we infer that the periphery of calderas reveals important information on the mechanisms of caldera formation and the structure of the underlying caldera floor.

ACKNOWLEDGMENTS

We thank B. Wenskowski and M. Sumita for help in the field, N. Urbanski for cooperation in the experimental setup, J. Stix, P. Lipman, R. Seyfried, L. Schwarzkopf, C. Schirnick, and S. Krastel for discussion, and O. Roche and an anonymous referee for constructive criticism. Grants from the Studienstiftung des Deutschen Volkes to Troll and from the Deutsche Forschungsgemeinschaft to Schmincke (Schm-250/72-1 and Schm-250/77-1) are gratefully acknowledged.

REFERENCES CITED

- Acocella, V., Cifelli, F., and Funicello R., 2000, Analogue models of collapse calderas and resurgent domes: *Journal of Volcanology and Geothermal Research*, v. 104, p. 81–96.
- Bogaard, P., and Schmincke, H.-U., 1998, Chronostratigraphy of Gran Canaria, in Weaver P.P.E., et al., *Proceedings of the Ocean Drilling Program, Scientific results, Volume 157: College Station, Texas, Ocean Drilling Program*, p. 127–140.
- Druitt, D.H., and Sparks, R.S.J., 1984, On the formation of calderas during ignimbrite eruptions: *Nature*, v. 310, p. 679–681.
- Freundt, A., and Schmincke, H.-U., 1995, Petrogenesis of rhyolite-trachyte-basalt composite ignimbrite P1, Gran Canaria, Canary Islands: *Journal of Geophysical Research*, v. 100, p. 455–474.
- Gardeweg, M., and Ramirez, C.F., 1987, La Pacana caldera and Atana Ignimbrite—A major ash flow and resurgent caldera complex in the Andes of northern Chile: *Bulletin of Volcanology*, v. 49, p. 547–566.
- Gudmundsson, A., 1988, Formation of collapse calderas: *Geology*, v. 16, p. 808–810.
- Henry, C., and Price, J., 1989, The Christmas Mountains caldera complex, Trans-Pecos Texas: *Bulletin of Volcanology*, v. 52, p. 97–112.
- Hubbert, M., 1951, Mechanical basis for certain familiar geologic structures: *Geological Society of America Bulletin*, v. 62, p. 355–372.
- Komuro, H., 1987, Experiments on cauldron formation: A polygonal cauldron and ring fractures: *Journal of Volcanology and Geothermal Research*, v. 31, p. 139–149.
- Krantz, R.W., 1991, Normal fault geometry and

- fault reactivation in tectonic inversion experiments, in Roberts et al., eds., *The geometry of normal faults: Geological Society [London] Special Publication 56*, p. 219–229.
- Krastel, S., and Schmincke, H.-U., 2001, Crustal structure of northern Gran Canaria deduced from active seismic tomography: *Journal of Volcanology and Geothermal Research* (in press).
- Lipman, P.W., 1997, Subsidence of ash-flow calderas: Relation to caldera size and chamber geometry: *Bulletin of Volcanology*, v. 59, p. 198–218.
- Marti, J., Ablay, G.J., Redshaw, L.T., and Sparks, R.S.J., 1994, Experimental studies of collapse calderas: *Geological Society [London] Journal*, v. 151, p. 919–929.
- Marti, J., Folch, A., Neri, A., and Macedonio, G., 2000, Pressure evolution during explosive caldera-forming eruptions: *Earth and Planetary Science Letters*, v. 175, p. 275–287.
- Nappi, G., Renzulli, A., and Santi P., 1991, Evidence of incremental growth in the Vulsinian calderas (central Italy): *Journal of Volcanology and Geothermal Research*, v. 47, p. 13–31.
- Newhall, C., and Dzurisin, D., 1988, Historical unrest at large calderas of the world: *U.S. Geological Survey Bulletin*, v. 1855, p. 1–1108.
- Roche, O., Druitt, T., and Merle, O., 2000, Experimental study of caldera formation: *Journal of Geophysical Research*, v. 105, p. 395–416.
- Schirnick, C., 1996, Formation of an intracaldera cone sheet dike swarm (Tejeda caldera, Gran Canaria) [Ph.D. thesis]: Kiel, Christian-Albrechts-Universität Kiel, p. 204.
- Schirnick, C., Bogaard, P., and Schmincke, H.-U., 1999, Cone sheet formation and intrusive growth of an ocean island—The Miocene Tejeda complex on Gran Canaria, Canary Islands: *Geology*, v. 27, p. 207–210.
- Schmincke, H.-U., 1967, Cone sheet swarm, resurgence of Tejeda caldera, and the early geologic history of Gran Canaria: *Bulletin of Volcanology*, v. 31, p. 153–162.
- Schmincke, H.-U., 1976, The geology of the Canary Islands, in Kunkel, G., ed., *Ecology and biogeography in the Canary Islands: The Hague, Netherlands, Junk B.V.*, p. 67–184.
- Schmincke, H.-U., and Swanson, D.A., 1966, Eine alte Caldera auf Gran Canaria: *Neues Jahrbuch für Geologie und Paläontologie*, v. 5, p. 260–269.
- Smith, R., and Bailey, R., 1968, Resurgent cauldrons, in *Studies in volcanology: A memoir in honor of Howel Williams: Geological Society of America Memoir 116*, p. 83–104.
- Troll, V.R., Emeleus, C.H., and Donaldson, C.H., 2000, Caldera formation in the Rum central igneous complex, Scotland: *Bulletin of Volcanology*, v. 62, p. 301–317.
- Varnes, D., 1963, *Geology and ore deposits of the South Silverton mining area, San Juan County, Colorado: U.S. Geological Survey Professional Paper 378-A*, p. 1–56.
- Walter, T.R., and Troll, V.R., 2001, Formation of caldera periphery faults, an experimental study: *Bulletin of Volcanology*, v. 63, p. 191–203.
- Ye, S., Rihm, R., Dañoibeitia, J., Canales, J., and Gallart, J., 1999, A crustal transect through the northern and northeastern part of the volcanic edifice of Gran Canaria: *Journal of Geodynamics*, v. 28, p. 3–26.

Manuscript received July 19, 2001
 Revised manuscript received October 8, 2001
 Manuscript accepted October 24, 2001

Printed in USA